

A New Parametrization of the Rain Drop Size Distribution

Ziad S. Haddad ¹,
David A. Short ²,
Stephen L. Durden ¹,
Eastwood 1111 ¹,
Scott Hensley ¹,
Martre B. Grable ¹,
and
Robert A. Black ³.

January 25, 1996

¹Jet Propulsion Laboratory, California Institute of Technology, Pasadena CA

²NASA Goddard Space Flight Center, Greenbelt MD

³NOAA AOML, Miami FL

Abstract

This paper revisits the problem of finding a parametric form for the rain drop size distribution (DSD) which 1) is an appropriate model for tropical rainfall, and 2) involves statistically independent parameters. Using TOGA/COARE data, we derive a parametrization which meets these criteria. This new parametrization is an improvement on the one that was derived in [3], using TRMM ground truth data from Darwin, Australia. The new COARE data allows us to verify that the spatial variability of the two “shape” parameters is relatively small, thus confirming that this parametrization should be particularly useful for remote sensing applications. We also derive new DSD-based radar-reflectivity-rain-rate power laws, whose coefficients are directly related to the shape parameters of the DSD. Perhaps most important, since the coefficients are independent of the rain-rate itself, and vary little spatially, the relations are ideally suited for rain retrieval algorithms. It should also prove straightforward to extend this method to the problems of estimating cloud hydrometeors from remote-sensing measurements.

1 Introduction

Rain drop size distribution (DSD) data obtained near Darwin, Australia, during the southern-hemisphere summer seasons of 1988-1989 and 1989-1990 have confirmed that the three parameters N_0 , μ and Λ in the Γ -distribution model

$$N(D)dD = N_0 D^\mu e^{-\Lambda D} dD \quad \text{drops of diameter } D \text{ mm, per m}^3 \quad (1)$$

that had been proposed by Ulbrich ([13]) are not mutually independent ([3]). In practice, this makes the representation (1) tricky to handle, mainly because without statistical independence one can easily make the wrong inferences from remote-sensing measurements about the DSD parameters. One particular derivation has been mis-used by so many authors so frequently that it deserves special mention: suppose two quantities Z (e.g. the radar reflectivity) and M (e.g. the total water mass) are related to the DSD (1) by equations $Z = a_Z \int_0^\infty D^{n_Z-1} N(D)dD$ and $M = a_M \int_0^\infty D^{n_M-1} N(D)dD$, so that after carrying out the integrations and “eliminating Λ ”,

$$Z = \frac{\Gamma(\mu + n_Z) a_Z N_0^{1 - (\mu + n_Z)/(\mu + n_M)}}{(\Gamma(\mu + n_M) a_M)^{(\mu + n_Z)/(\mu + n_M)}} M^{(\mu + n_Z)/(\mu + n_M)} \quad (2)$$

The illogical step is to then decide that whenever one comes across another equality

$$Z = \alpha M^\beta, \quad (3)$$

one can automatically conclude that

$$\alpha = \frac{\Gamma(\mu + n_Z) a_Z N_0^{1 - (\mu + n_Z)/(\mu + n_M)}}{(\Gamma(\mu + n_M) a_M)^{(\mu + n_Z)/(\mu + n_M)}} \quad \text{and} \quad \beta = \frac{\mu + n_Z}{\mu + n_M}. \quad (4)$$

This is of course not correct: for example, (3) could just as easily be satisfied with

$$\alpha = \frac{10 \Gamma(\mu + n_Z) a_Z N_0^{1 - (\mu + n_Z)/(\mu + n_M)}}{(\Gamma(\mu + n_M) a_M)^{(\mu + n_Z)/(\mu + n_M)}} \quad \text{and} \quad \beta = \frac{\mu + n_Z}{\mu + n_M} - \frac{\log(10)}{\log(M)}, \quad (5)$$

or with

$$\alpha = \frac{\Gamma(\mu + n_Z) a_Z N_1^{1 - (\mu + n_Z)/(\mu + n_M)}}{(\Gamma(\mu + n_M) a_M)^{(\mu + n_Z)/(\mu + n_M)}} \quad \text{and} \quad \beta = c + (1 - c) \frac{\mu + n_Z}{\mu + n_M} \quad (6)$$

(if N_0 and M were related by a power law $N_0 = N_1 M^c$ with N_1 and c new parameters replacing N_0), or indeed with an infinite number of radically different possibilities, each implying drastically differing behaviors for α and β . The point is that, in order to make a conclusion such as (4), one must postulate not just that equation (3) holds, but also that the exponent and M in (2) and (3) are mutually independent, and that the linear factor and M are too. Thus, one would need to know that N_0 and M are independent, and that μ and

M are independent, or one would have to replace them via parameters that are. Failure do so renders one's conclusions dubious at best, in any case unsubstantiated.

The re-parametrization

$$\mu = \frac{c_{0.034R^{0.74}}}{s'^2 D^{0.4}} \cdot A \quad (7)$$

$$\Lambda = \frac{c_{0.034R^{0.74}}}{s'^2 D^{1.4} \bar{R}^{0.155}} \quad (8)$$

$$N_0 = \frac{55 \cdot \Gamma(\cdot, \bar{A})}{\Gamma(\cdot, \bar{A})} A^{\mu+4} + 0.53/\Lambda \quad (9)$$

derived in [3] using the Darwin data, is useful precisely because it involves the statistically independent parameters R (the rain rate), s' and D' . The parameter D' is essentially a "normalized" version of the mass-weighted mean drop diameter D^* , to which it is related by the formula $D^* = D' R^{0.155}$. The other DSD "shape" parameter s' is related to the mass-weighted relative r.m.s. spread s^* of the drop diameters by $s^* = s' D^{*0.2} R^{-0.031} c_{0.0172 R^{0.74}}$. Unfortunately, the Darwin data exhibited apparently anomalous behavior for larger rain rates, namely a sudden non-zero correlation between s^* and R when the rainrate exceeded 12 mm/hr ([3, fig. 1c]), a correlation which was negligible when the condition $R < 10$ mm/hr was imposed, and which is responsible for the exponential terms in (7)–(9). Since those data were collected using a Joss-Waldvogel disdrometer ([5]), an instrument which has been shown to be non-stationary, especially when exposed to higher rain rates ([12]), an analysis of DSD measurements from other tropical locations using different instruments was clearly necessary to verify the Darwin results. The TOGA/COARRJ data allowed us to do just that. Collected in the warm pool of the western equatorial Pacific between November, 1992, and February, 1993 ([9]), using NCAR's 2-D PMS spectrometer probes mounted on the NCAR Electra aircraft ([2, 14]), these data also made it possible for the first time to estimate the correlation length of the DSD shape parameters. Section 2 describes the results of the data analysis. In section 3, we use these results to derive simple new relations between the radar reflectivity coefficient Z_e and the rain rate R for a given DSD).

2 Statistical analysis of the TOGA/COARRJ data

The NCAR 2-D PMS spectrometer probe data were reduced using a method essentially similar to the one described in [2]. The measurements were so exceptionally defect-free that the partial-image rejection criteria of [2] were extensively altered to accept most partial images. In order to fit a model such as (1) to each of the sampled DSDs, one could (A) use a moment method (MM) to calculate (N_0, μ, Λ) ; (B) find those values of (N_0, μ, Λ) that minimize the m.s. distance between (1) and the measured histograms; or (C) apply a maximum-likelihood method as in [3]. Because method A produces notoriously biased

estimates, often with large variances, and because method B implicitly makes the unnecessary over-simplification that the difference between the observation and the model is entirely due to Gaussian white noise evenly spread among the sampling bins, we opted for method C.

As in [3], instead of N_0 , μ and Λ , we used the more physically meaningful parameters

$$D^* = \text{mass-weighted mean drop diameter} = \frac{\mu + 4}{\Lambda} \text{ mm} \quad (10)$$

$$s^* = \text{relative mass-weighted r.m.s. deviation of the drop diameters} = \frac{1}{\sqrt{\mu + 4}} \quad (11)$$

$$R = \text{instantaneous rain rate} = 6\pi \cdot 10^{-4} \int 9.65 (1 - e^{-0.53D}) D^3 N_0 D^\mu e^{-\Lambda D} dD \quad (12)$$

$$00182 \cdot \frac{\Gamma(\mu + 4)}{\Lambda^{\mu+4}} \left(\mathbf{1} - (1 + 0.53/\Lambda)^{-\mu} \right) N_0 \text{ mm/hr} \quad (13)$$

The estimates obtained are shown in the pairwise-scatter diagrams of figure 1. Since the estimates of D^* and s^* obtained during very light rain can be unreliable because of the small sample size, we imposed a lower-bound condition on R . The particular value of 0.7 mm/hr was chosen because it corresponds to the projected Tropical Rainfall Measuring Mission (TRMM) radar's sensitivity ([6, 10]). This lower-bound was exceeded by 8040 samples. The sample mean of D^* was 1.11 mm, with a standard deviation of 0.41 mm. The sample mean of s^* was 39.6 %, with a standard deviation of 3.8 %. The values of the various conditional correlation coefficients (conditioned on $R > 0.7$ mm/hr) are given in table 1. The COARE mean drop diameter is thus significantly smaller than the 1.82-mm estimate corresponding to the Darwin data, a fact which is consistent with the Darwin disdrometer under-estimating the smaller drops at higher rainrates ([12]). More significant is the fact that the negative correlations observed at Darwin between s^* on one hand and R and D^* on the other are not confirmed. Indeed, figure 1b shows quite clearly that the anomalous negative correlation between s^* and R at the higher rainrates which was observed in the Darwin data is reassuringly not present in the COARE observations.

To construct mutually uncorrelated parameters, we proceed as in [3]. Rather than use power-law regressions and, for example, express N_0 as $N_0 = a\mu^b$ or Λ as $\Lambda = cR^d$ then try to determine bounds for the artificially-introduced parameters a , b , c and d , we look for a judicious change of variables mapping the parameters (R, D^*, s^*) onto a new triple of uncorrelated variables (R, D'', s'') . Since the joint behavior of R and D^* is not significantly different between the Darwin data and the COARE data, we shall let $D'' = D'$, i.e.

$$D'' = D^* R^{-0.155} \quad (14)$$

To determine s'' , we first define an intermediate variable \hat{s} which we force to be uncorrelated with R . Thus

$$\log(s^*) = \log(\hat{s}) + \beta \log(R) \quad (15)$$

and we require that β satisfy

$$\mathcal{E}\{\log(s^*)\log(R)\} = \beta \mathcal{E}\{\log(R)^2\} = \mathcal{E}\{\log(s^*)\}\mathcal{E}\{\log(R)\} + \beta \mathcal{E}\{\log(R)\}^2 \quad (16)$$

Using the COARE data to compute the moments in (10), one finds that

$$\beta = 0.037 \quad (17)$$

We then replace \hat{s} by that variable s'' which is uncorrelated with either R or D'' . Thus

$$\log(\hat{s}) = \log(s'') + \gamma \log(D'') \quad (18)$$

and s'' will be automatically uncorrelated with R (because \hat{s} and D'' are), so it suffices to choose γ in such a way that s'' and D'' are uncorrelated. Proceeding as before, one finds

$$\gamma = 0.165 \quad (19)$$

Thus our three uncorrelated variables are

$$R = \text{instantaneous rain rate} \quad (20)$$

$$D'' = D \cdot R^{0.155} \quad (21)$$

$$\text{and } s'' = s \cdot D^{0.165} R^{0.0114} \quad (22)$$

The scatter diagrams in figure 2 show the values of these new variables for the COARE 1) SDs. The marginal statistics for each individual variable are summarized in table 2. The table also shows the marginal statistics of D'' and s'' for the Darwin data, conditioned on $R < 12 \text{ mm/hr}$ then unconditional. It is quite encouraging to note that the conditional statistics at Darwin are indeed quite similar to the COARE results. Note the very small standard deviation for the parameter s'' . Table 3 confirms that the correlation coefficients are all negligibly small, for the COARE data as well as the conditioned Darwin data. In particular, one can conclude from these tables that the joint and marginal statistics of the new DSD shape parameters D'' and s'' are much the same in altitude as at the surface. The expressions for the original DSD parameters in (1) in terms of $\{\mu, \Lambda, N_0, s''\}$ are

$$\mu = \frac{1}{s''^2 \Lambda^{0.33} R^{0.074}} - 4 \quad (23)$$

$$\Lambda = \frac{1}{s''^2 \Lambda^{0.33}} \{0.23\} \quad (24)$$

$$N_0 = 55 \frac{\Lambda^{\mu+4}}{\Gamma(\mu+4) (1 - 0.53/\Lambda)^{\mu-4}} R \quad (25)$$

The COARE data allows us to estimate the spatial variability of the $\{\mu, \Lambda, N_0\}$ parameters. Two measures of variability are particularly useful: the auto correlation coefficient, ρ_δ , and the relative m.s. variation v_δ , defined for a stationary random process X_t by

$$v_\delta = \frac{\mathcal{E}\{(X_t - X_{t+\delta})^2\}}{\sqrt{\mathcal{E}\{X_t^2\} \cdot \mathcal{E}\{X_{t+\delta}^2\}}} \quad \left(= \frac{\mathcal{E}\{(X_t - X_{t+\delta})^2\}}{\mathcal{E}\{X_t^2\}} \text{ ideally} \right) \quad (26)$$

Table 4 shows the values obtained from the COARE data when X was R , then D'' , then N_0 . The sample size was insufficient to calculate correlations beyond $\delta = 8 \text{ km}$ with much confidence. The results confirm that the spatial variation of D'' remains quite small indeed. Note that table 4 does not show the spatial auto correlation statistics of s'' because the standard deviation of s'' (over the entire data) is already a quite small $0.025/0.3 = 6.41 \text{ O}'$.

3 Application

Weather radars can measure the effective reflectivity Z_e of rainfall quite accurately (see, e.g., [1]). At higher frequencies, such as the 13.8 GHz frequency of the TRMM radar, the measured reflectivity is lower than the true Z_e because of the attenuation $\int_{\gamma} k$ accumulated along the propagation path γ , where k is the attenuation coefficient. The problem of estimating R given attenuated reflectivity measurements can be expressed using Z - R and k - R relations. Naturally, there are numerous Z - R and k - R relations for any given frequency ([11]), ultimately depending on the shape of the drop size distribution, and, to a lesser extent, on other environmental factors. Choosing the wrong relations can lead to serious errors in the retrieved rainfall. That is why several investigators have developed DSD-based retrieval algorithms (e.g. [4], [7], [8]). The results of section 2, in particular (23)–(25), are directly applicable to these algorithms. Specifically, these formulas should allow one to avoid the inconsistency of assuming μ and/or N_0 constant and letting Λ vary when in fact the three variables are significantly correlated. Indeed, it is entirely consistent to make the corresponding assumptions about the uncorrelated variables s'' , D'' and R .

To obtain power-law relations between Z_e and R and between k and R , we assigned to the pair (s'', D'') regularly-spaced discrete values in the range $0.34 < s'' < 0.44$, $0.7 < D'' < 1.8$: in each case, we used a 13.8-GHz Mie-scattering model to compute $Z_e(R)$ and $k(R)$ exactly as the rainrate R varied in the range $1 < R < 130$ mm/hr, assuming that the temperature had one of three values, 275 K, 282.5 K, or 290 K. The power law minimizing the sum of the mean-squared distances from the three Mie-calculated functions at the three nominal temperatures was then calculated for each pair. The resulting Z - R and k - R 13.8GHz power-law relations

$$Z_e = a(s'', D'')R^{b(s'', D'')} \quad (27)$$

$$k = \alpha(s'', D'')R^{\beta(s'', D'')} \quad (28)$$

are given in tables (5)–(8). To illustrate the validity of (27) and (28), figure 3 shows the Mie and approximate k - R and Z_e - R curves at 13.8 GHz, when $s'' = 0.44$ and $D'' = 1.8$. The power-law formula over-estimates Z by about 1.4 dB when $R = 1$ mm/hr, and the error decreases steadily as R increases. The approximate and exact k - R curves do not differ significantly in this case. At the other extreme, Figure 4 shows the Mie and approximate curves when $s'' = 0.34$ and $D'' = 0.8$, corresponding to smaller drops. The difference between the power-law formula estimates of k and its Mie values is about 0.3 dB when $R = 150$ mm/hr, and the error decreases steadily as R decreases. The approximate and exact Z - R curves do not differ significantly in this case. A systematic analysis of the difference between the approximate formulas (27) and (28) and the exact Mie calculations at 275, 282.5 and 290 K was conducted for values of s'' and D'' in the intervals $0.34 \leq s'' \leq 0.44$ and $0.7 \leq D'' \leq 1.8$, and for rainrates between 1 and 130 mm/hr: (27) is never farther than 8.6% from the Mie-calculated dBZ values, the relative difference between (28) and the

Mie-calculated at tenuation coefficient never exceeds 9.8%, while the absolute error remains below 0.18 dB/km.

4 Conclusions

Based on the TOGA/COARE and Darwin data sets, one can parametrize drop-size distributions using the variables R , D'' and s'' defined above, and assume that these parameters are uncorrelated. The variance of the shape parameter s'' is relatively small, and the auto-decorrelation lengths of D'' and of s'' are sufficiently large that one can reasonably assume that D'' and s'' remain constant over several kilometers. These properties make this parametrization particularly useful in remote sensing retrieval problems.

5 Acknowledgements

We wish to thank David Atlas for many fruitful discussions. This work was performed at the Jet Propulsion Laboratory, California Institute of Technology, under contract with the National Aeronautics and Space Administration.

References

- [1] Atlas, D. A., editor, **J 990**: Radar in Meteorology: Battan Memorial and 40th Anniversary Radar Meteorology Conference. Boston: American Meteorological Society.
- [2] Black, R. A., and Hallett, J., **1986**: Observations of the distribution of ice in hurricanes, *J. Atmos. Sci.* **43**, 802-822.
- [3] Haddad, Z. S., Durden, S. I., and Im, E., **1996**: Parametrizing the raindrop size distribution, *J. Appl. Meteor.* **35**, 3-13.
- [4] Haddad, Z. S., Im, E., Durden, S. I., and Hensley, S., **1996**: Stochastic filtering of rain profiles using radar, surface-referenced radar, or combined radar-radiometer measurements, *J. Appl. Meteor.* **35**, ?-?.
- [5] Loss, J., and Waldvogel, A., **1967**: A raindrop spectrograph with automatic analysis, *Pure Appl. Geophys.*, **68**, 240-246.
- [6] Kawanishi, J., Takamatsu, H., Kozu, T., Okamoto, K., and Kumagai, H., **1993**: TRMM precipitation radar, *Preprints IGARSS '93*, 423-425.

- [7] Koizu, T., Nakamura, K., Meneghini, R., and Bonczyk, W.C., **1991**: Dual-parameter radar rainfall measurement from space: A test result from an aircraft experiment, *IEEE Trans. Geosci. Remote Sensing* **29**, 690-703.
- [8] Kumagai, H., Meneghini, R., and Nakamura, K., **1993**: Combined analysis of airborne single-frequency radar and multi-frequency radiometer observations in the TRMM 1 experiment, *Proc. 26th Intl. Conf. Radar Meteor.*, 696-698.
- [9] Lukas, R., Webster, P.J., Ji, M., and Leetmaa, A., **1995**: The large-scale context for the TOGA Coupled Ocean-Atmosphere Response Experiment, *Meteor. Atmos. Phys.* **56**, 3-16.
- [0] Okamoto, K., Awaka, J., and Koizu, T., **1988**: A feasibility study of rain radar for the tropical rainfall measuring mission: 6. A case study of rain radar system, *J. Comm. Research Lab.* **35**, 183-208.
- 1 Olsen R., Rogers, D., and Hodge, D., **1978**: The dBZ relation in the calculation of rain attenuation *IEEE Trans. Ant. Prop.* **26**, 318-329.
- 2] Seppard, I. E., and Joe, P.J. = **994**. Comparison of raindrop size distribution measurements by a Joss-Waldvogel disdrometer, a PMS 2D-G spectrometer, and a POSS Doppler radar, *J. Atmos. Oceanic Technol.* **1**, 874-887.
- 13 Ulbrich, C.W., **1983**: Natural variations in the analytical form of the raindrop size distribution, on computer simulations of dual-measurement radar methods *J. Climate Appl. Meteor.*, **22**, 1764-1775.
- [4 Yuter, S.F., Houze, R.A., Small, B.F., Marks, F.D., Daugherty, J.R., and Brodzik, S.R., **1995**: TOGA COARE aircraft mission summary images - an electronic atlas, *Bull. Amer. Meteor. Soc.* **76**, 319-328.

Figure captions

Figure 1: Scatter diagrams for the COARE observations: (a) (R, D^*) pairs; (b) (D^*, s^*) pairs; (c) (R, s^*) pairs.

Figure 2: Scatter diagrams for the COARE estimates: (a) (R, D'') pairs; (b) (D'', s'') pairs; (c) (R, s'') pairs.

Figure 3: Exact Mic curves when the DSD parameters are $s' = 0.44$ and $D' = 1.8$, along with the graph of our power-law approximations: (a) $Z_c R$; (b) $k R$.

Figure 4: Exact Mic curves when the DSD parameters are $s' = 0.34$ and $D' = 0.8$, along with the graph of our power-law approximations: (a) $Z_c R$; (b) $k R$.

Variables	Correlation Coefficient
$\log(R)$ and $\log(D'')$	0.29
$\log(R)$ and $\log(s'')$	0.35
$\log(D'')$ and $\log(s'')$	0.72

Table 1: Correlation coefficients for the COARE data conditioned on $R > 0.7$ mm/hr.

	Mean		Standard Deviation	
	TOGA COARE	Darwin $R < 12$ mm/hr unconditional	TOGA COARE	Darwin $R < 12$ mm/hr unconditional
D''	0.92	1.38	0.32	0.34
s''	0.39	0.39	0.025	0.035
$\log(D'')$	-0.1	0.28	0.1	0.26
$\log(s'')$	-0.95	-0.94	0.068	0.099

Table 2: Marginal statistics of D'' and s'' conditioned on $R > 0.7$ mm/hr.

	TOGA COARE	$R < 12$ mm/hr unconditional
$\log(R)$ and $\log(D'')$	$-1.4 \cdot 10^{-1}$	$8.64 \cdot 10^{-3}$ /hr
$\log(R)$ and $\log(s'')$	$7.6 \cdot 10^{-2}$	$-1.4 \cdot 10^{-1}$
$\log(D'')$ and $\log(s'')$	$4.9 \cdot 10^{-2}$	$-5.0 \cdot 10^{-2}$

Table 3: Correlation coefficients of R , D'' and s'' , conditioned on $R > 0.7$ mm/hr.

δ (h)	Relative m.s. Variation			Correlation Coefficient			Sample size
	R	D''	$\log(N_0)$	R	D''	$\log(N_0)$	
1	21.7%	1.84%	3.9%	0.846	0.91	0.85	7081
2	39.1%	3.12%	6.1%	0.722	0.84	0.742	6610
3	53.0%	3.76%	6.98%	0.621	0.803	0.693	6227
4	65.2%	4.39%	7.57%	0.532	0.766	0.642	5904
5	74.2%	4.75%	8.1%	0.466	0.742	0.599	5616
6	80.7%	4.97%	8.21%	0.411	0.727	0.576	5358
7	83.9%	5.27%	8.67%	0.385	0.707	0.545	5121
8	87.2%	5.57%	9.22%	0.376	0.686	0.508	4909

Table 4: Spatial auto-correlation statistics of R , D'' and $\log(N_0)$, conditioned on $R > 0.7$ mm/hr.

$s'' \setminus D''$	0.7	0.8	0.9	1.0	1.1	1.2	1.3	1.4	1.5	1.6	1.7	1.8
0.31	68.83	89.67	118.49	159.63	217.44	296.37	400.83	534.98	702.44	905.99	1147.31	1426.86
0.36	70.32	93.02	125.22	171.44	236.23	324.22	439.88	587.25	769.57	989.02	1246.45	1541.32
0.38	72.19	97.12	133.16	185.01	257.46	355.28	482.92	644.19	841.81	1077.18	1350.21	1659.30
0.40	74.48	102.01	142.38	200.45	281.26	389.68	530.05	705.77	918.91	1169.96	1457.78	1779.67
0.42	77.27	107.85	152.99	217.90	307.78	427.55	581.30	771.89	1000.01	1266.74	1568.27	1901.36
0.44	80.59	114.61	165.06	237.45	337.15	468.98	636.66	842.32	1086.25	1366.85	1680.78	2023.29

Table 5: a as in $Z_c = aR^b$

$s'' \setminus D''$	0.7	0.8	0.9	1.0	1.1	1.2	1.3	1.4	1.5	1.6	1.7	1.8
0.34	1.413	1.471	1.497	1.508	1.505	1.492	1.472	1.447	1.419	1.390	1.359	1.329
0.36	1.444	1.480	1.501	1.507	1.499	1.483	1.459	1.432	-1.403	1.372	1.341	1.310
0.38	1.455	1.487	1.503	1.504	1.492	1.472	1.446	1.417	1.386	1.354	1.323	1.291
0.40	1.465	1.493	1.504	1.499	1.483	1.460	1.432	1.401	1.369	1.336	1.305	1.274
0.42	1.474	1.497	1.503	1.193	1.473	1.447	1.417	1.385	1.352	1.319	1.287	1.256
0.44	1.482	1.500	1.500	1.486	1.463	1.434	1.402	1.365	1.335	1.302	1.270	1.240

Table 6: b as in $Z_c = aR^b$

$s'' \setminus D''$	0.7	0.8	0.9	1.0	1.1	1.2	1.3	1.4	1.5	1.6	1.7	1.8
0.34	0.0162	0.0171	0.0188	0.0211	0.0239	0.0269	0.0300	0.0332	0.0362	0.0391	0.0420	0.0447
0.36	0.0164	0.0174	0.0193	0.0217	0.0245	0.0275	0.0306	0.0336	0.0366	0.0395	0.0423	0.0450
0.38	0.0167	0.0179	0.0198	0.0223	0.0251	0.0280	0.0311	0.0341	0.0370	0.0399	0.0426	0.0453
0.40	0.0170	0.0183	0.0203	0.0228	0.0256	0.0286	0.0316	0.0345	0.0374	0.0403	0.0430	0.0457
0.42	0.0173	0.0187	0.0208	0.0234	0.0262	0.0291	0.0321	0.0350	0.0379	0.0407	0.0434	0.0461
0.44	0.0177	0.0192	0.0214	0.0240	0.0268	0.0297	0.0326	0.0355	0.0384	0.0412	0.0439	0.0465

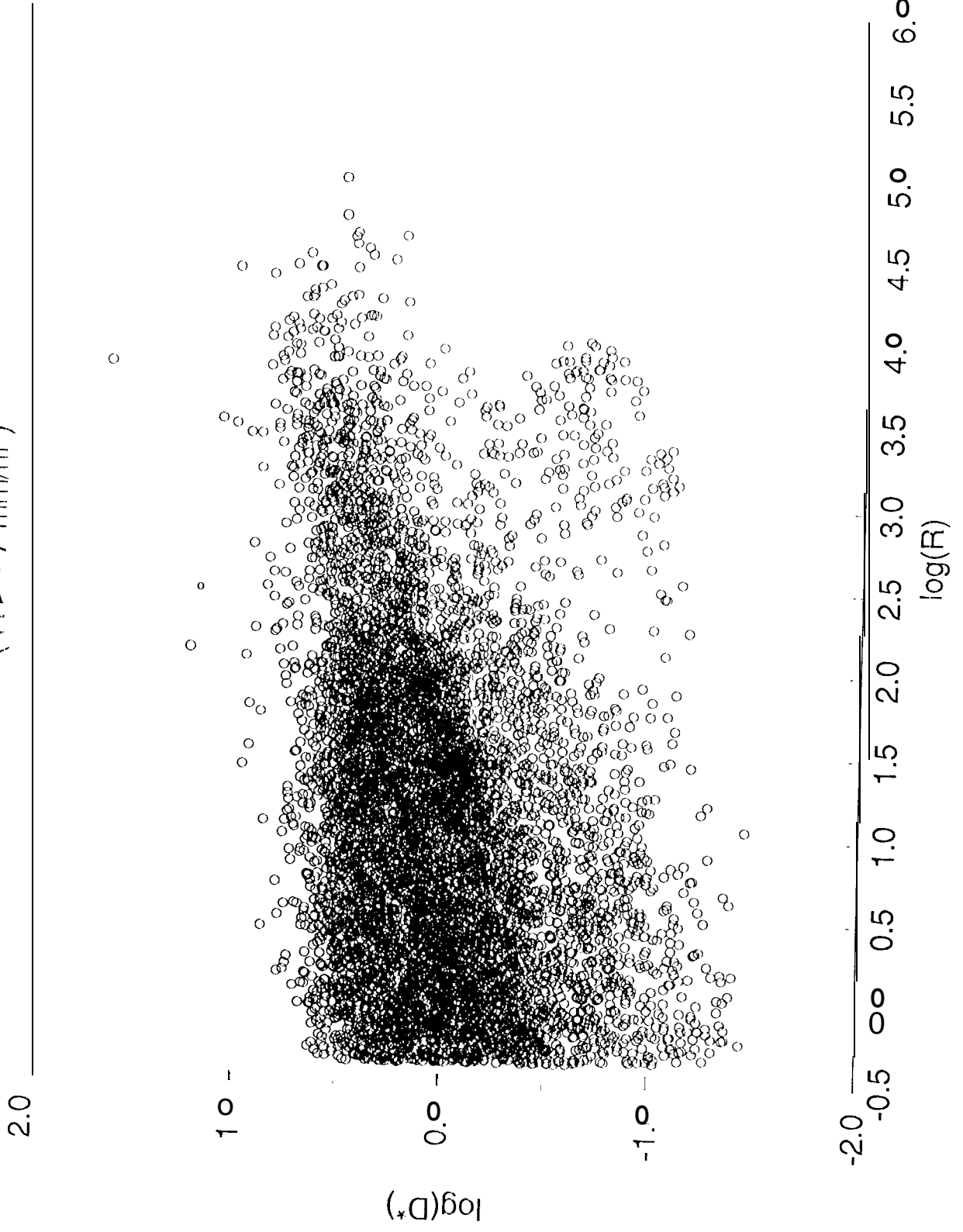
Table 7: α as in $k = \alpha R^\beta$

$s'' \setminus D''$	0.7	0.8	0.9	1.0	1.1	1.2	1.3	1.4	1.5	1.6	1.7	1.8
0.34	1.137	1.161	1.169	1.166	1.158	1.146	1.113	1.121	1.109	1.097	1.086	1.076
0.36	1.138	1.159	1.165	1.161	1.152	1.141	1.129	1.117	1.105	1.094	1.082	1.071
0.38	1.138	1.157	1.161	1.156	1.147	1.136	1.124	1.112	1.101	1.089	1.078	1.067
0.40	1.138	1.154	1.157	1.152	1.142	1.131	1.120	1.108	1.097	1.085	1.074	1.062
0.42	1.138	1.151	1.153	1.147	1.138	1.127	1.115	1.104	1.092	1.081	1.069	1.058
0.44	1.137	1.149	1.149	1.143	1.133	1.122	1.111	1.099	1.088	1.076	1.064	1.053

Table 8: β as in $k = \alpha R^\beta$

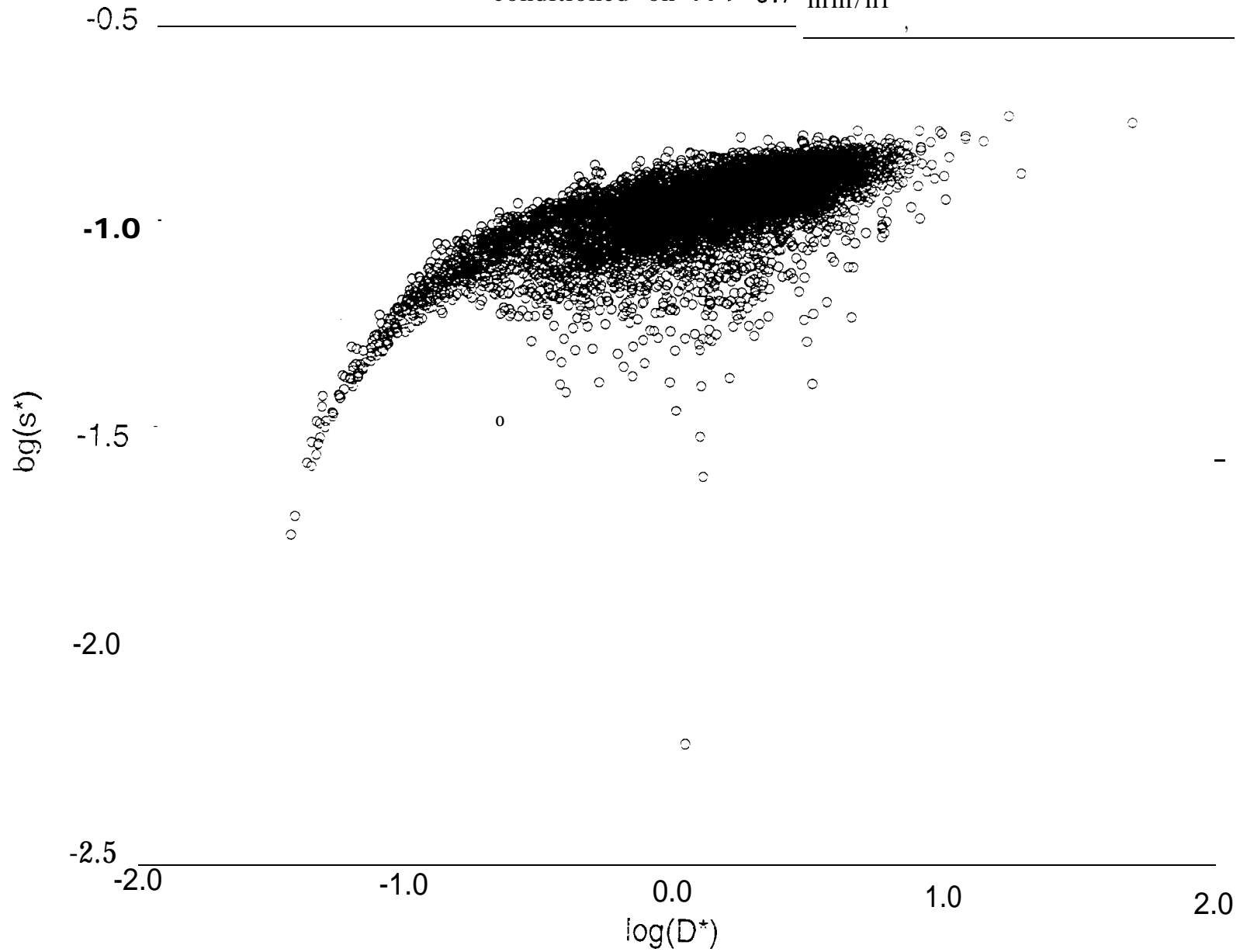
COARE

($R > 0.7$ mm/hr)



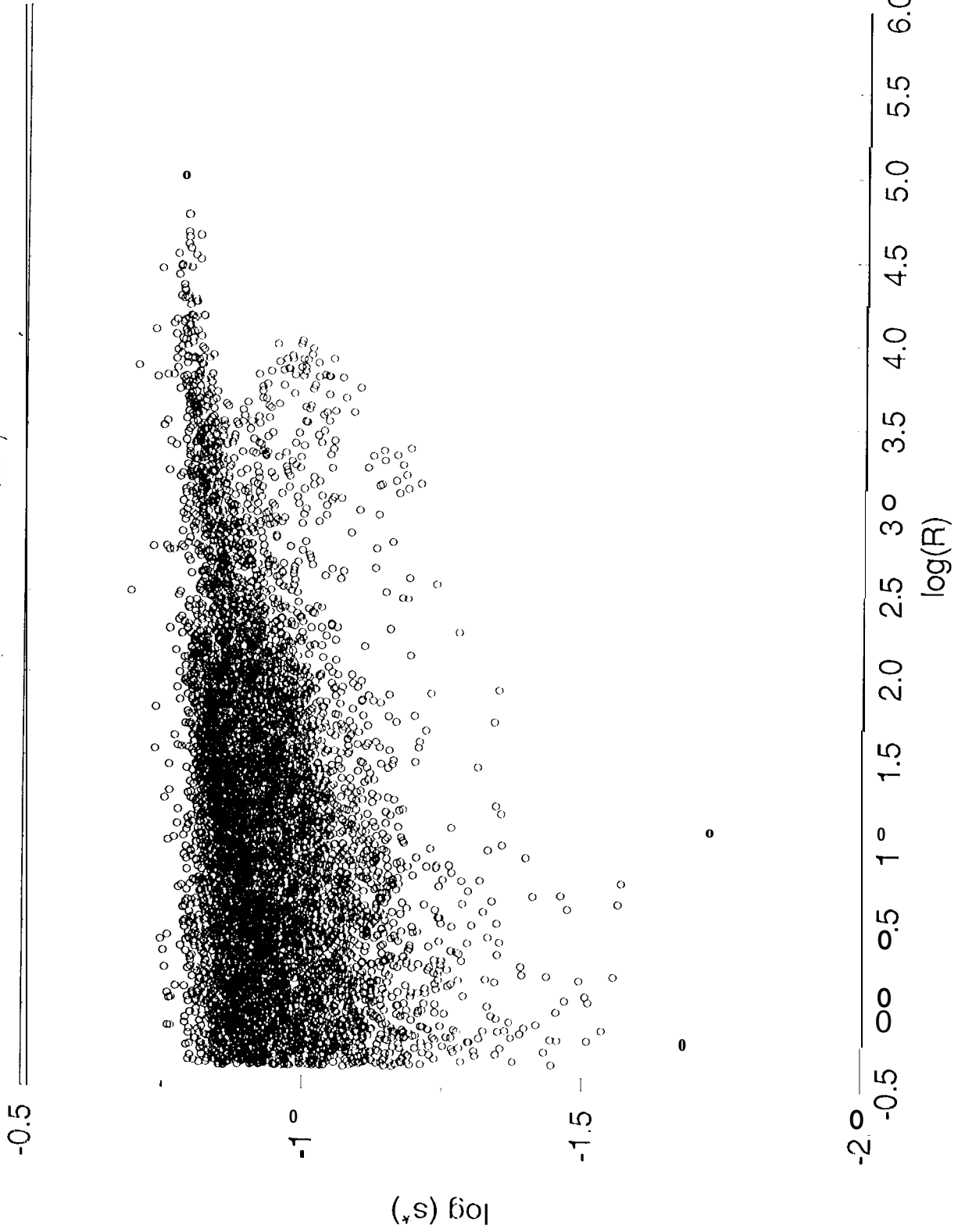
COARE

conditioned on $R > 0.7$ mm/hr



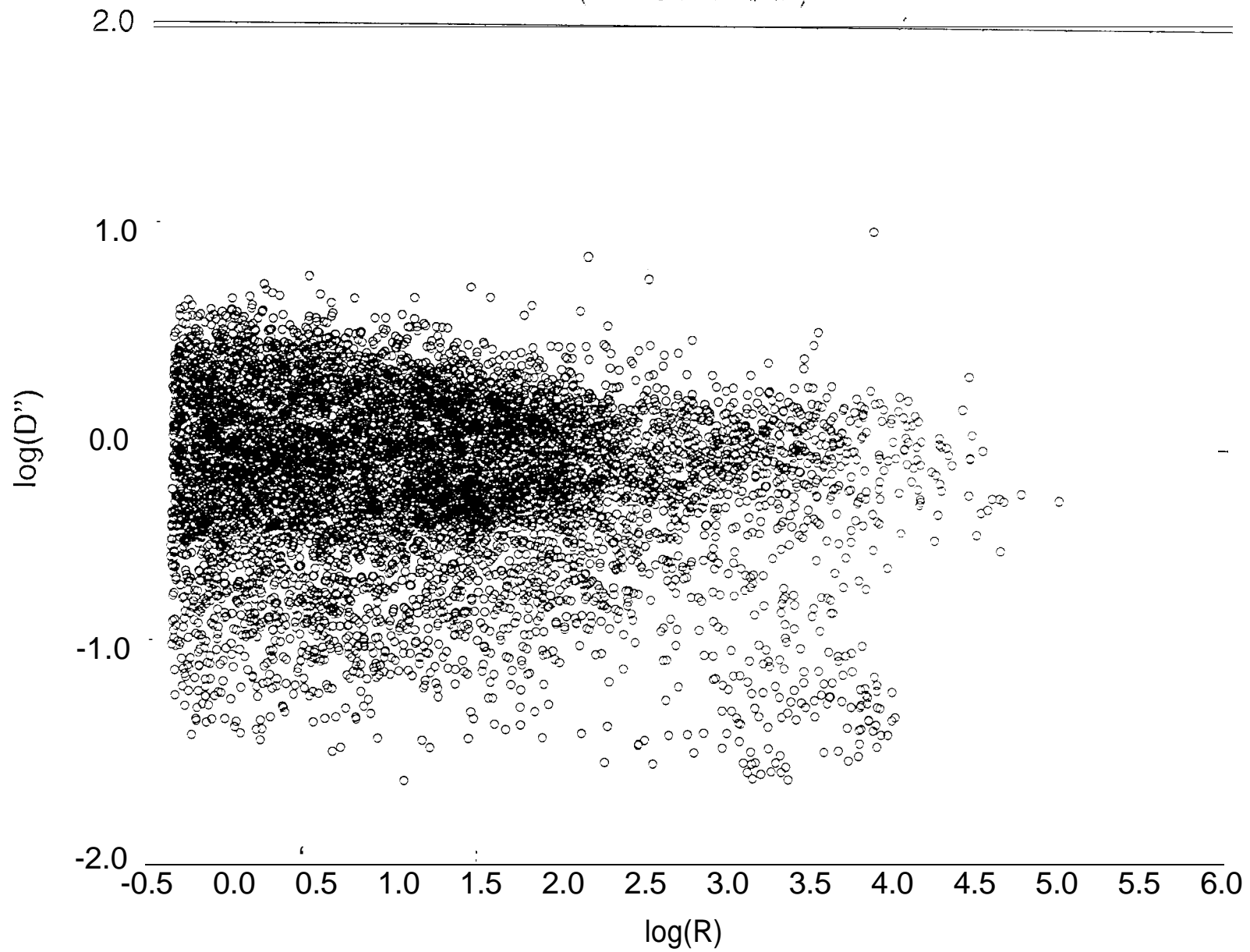
COARE

($R > 0.7$ mm/hr)



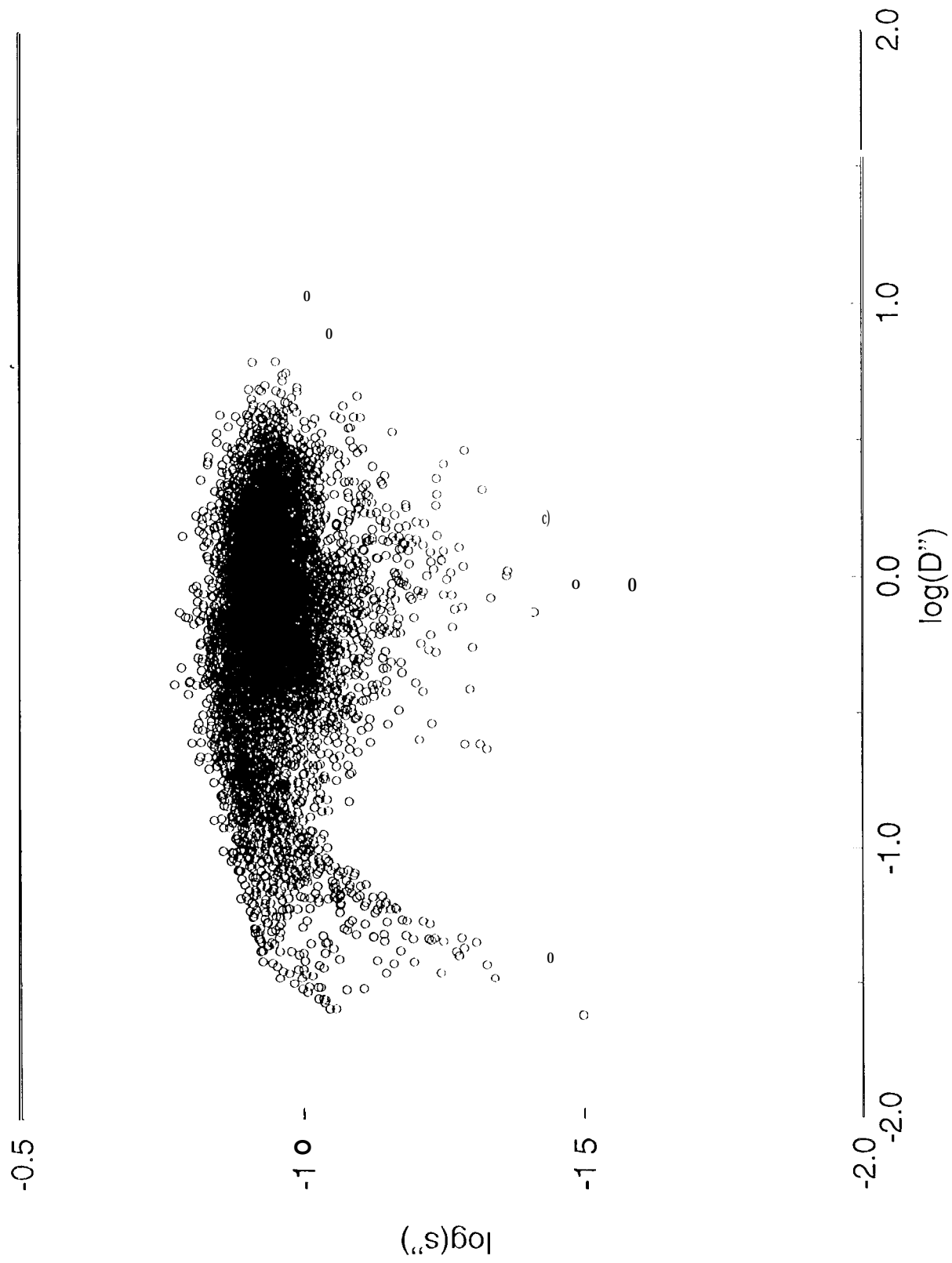
COARE

($R > 0.7$ mm/hr)



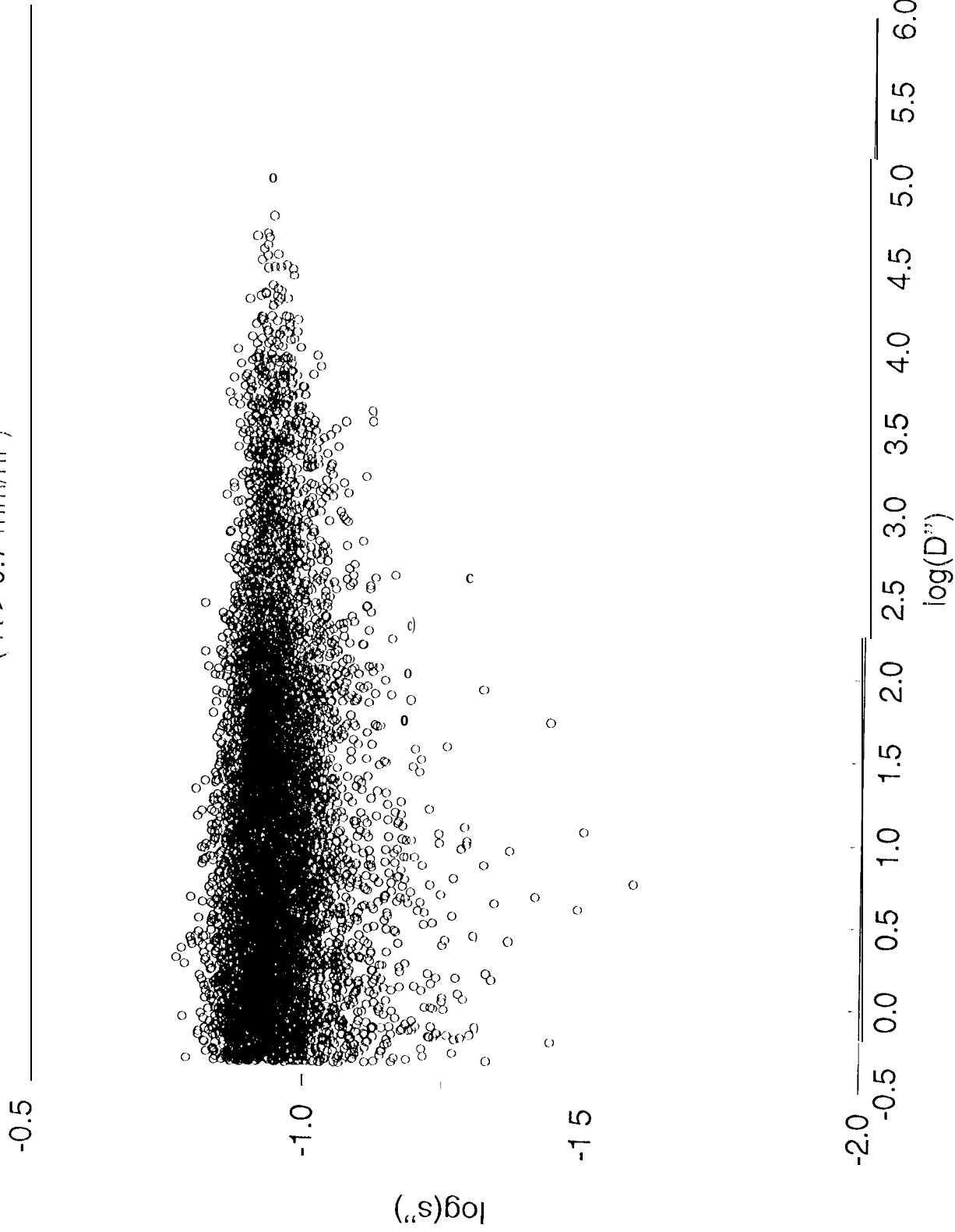
COARE

conditioned on $R > 0.7$ mm/hr



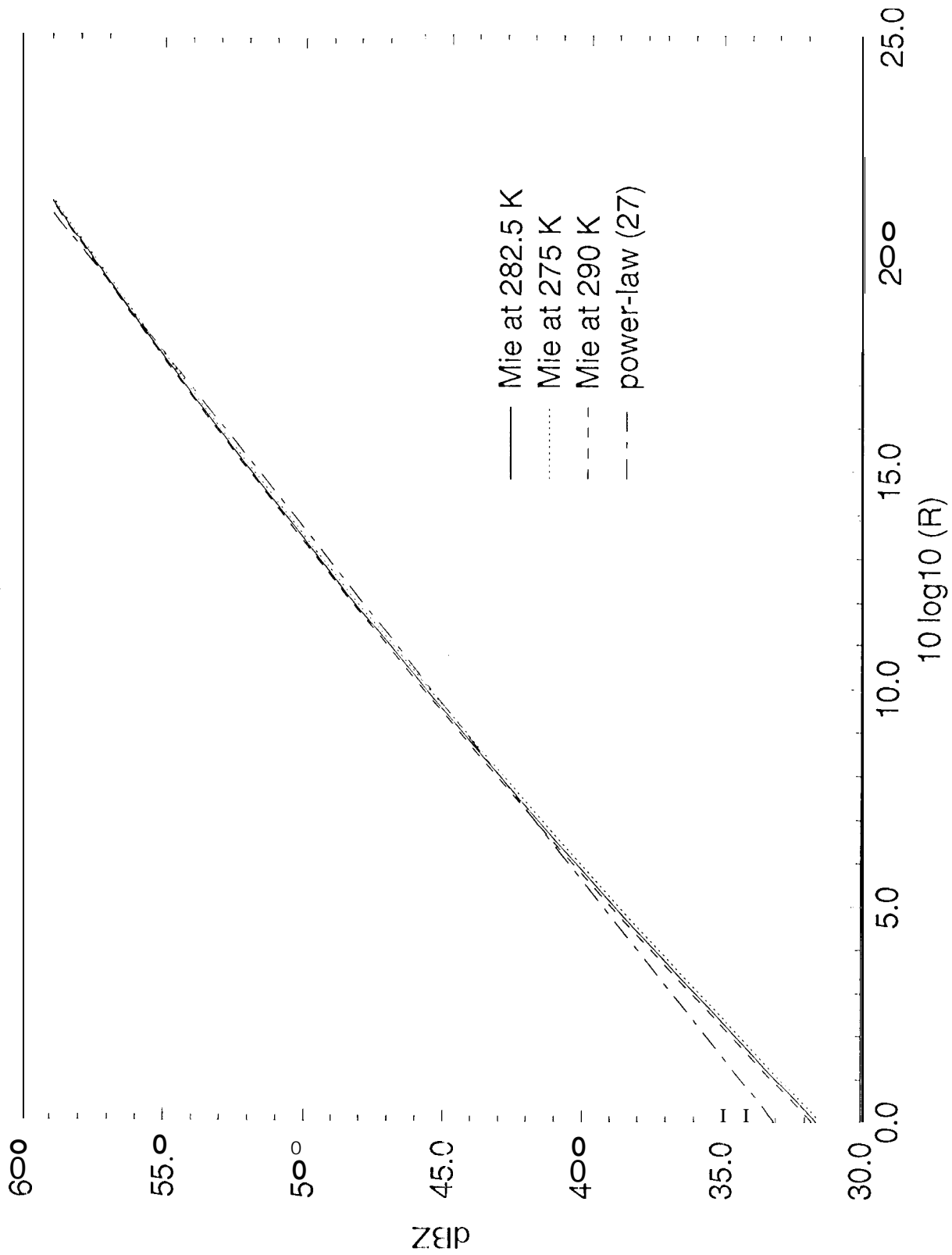
COARE

(R > 0.7 mm/hr)



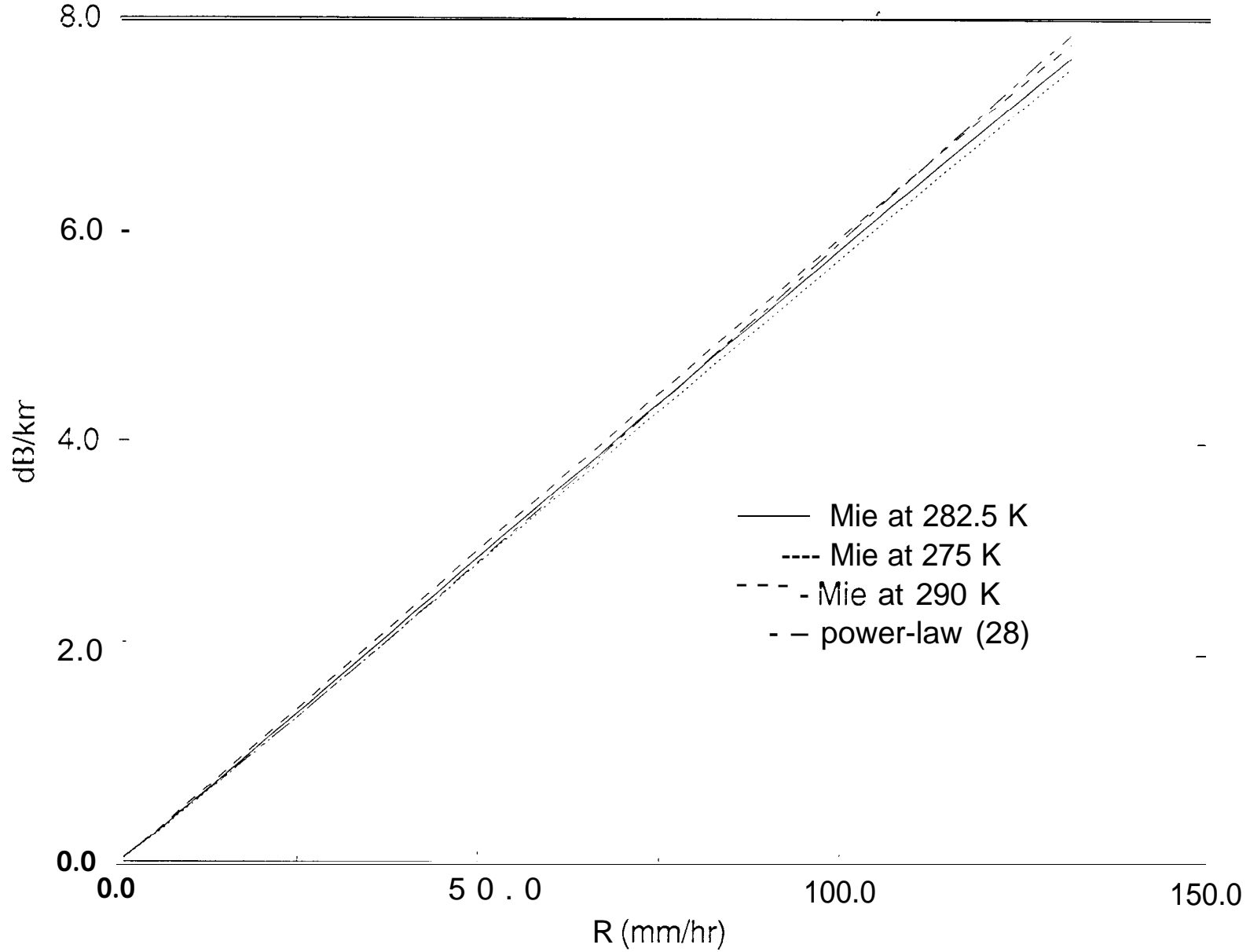
Z - R

$D''=1.8, s''=0.44$



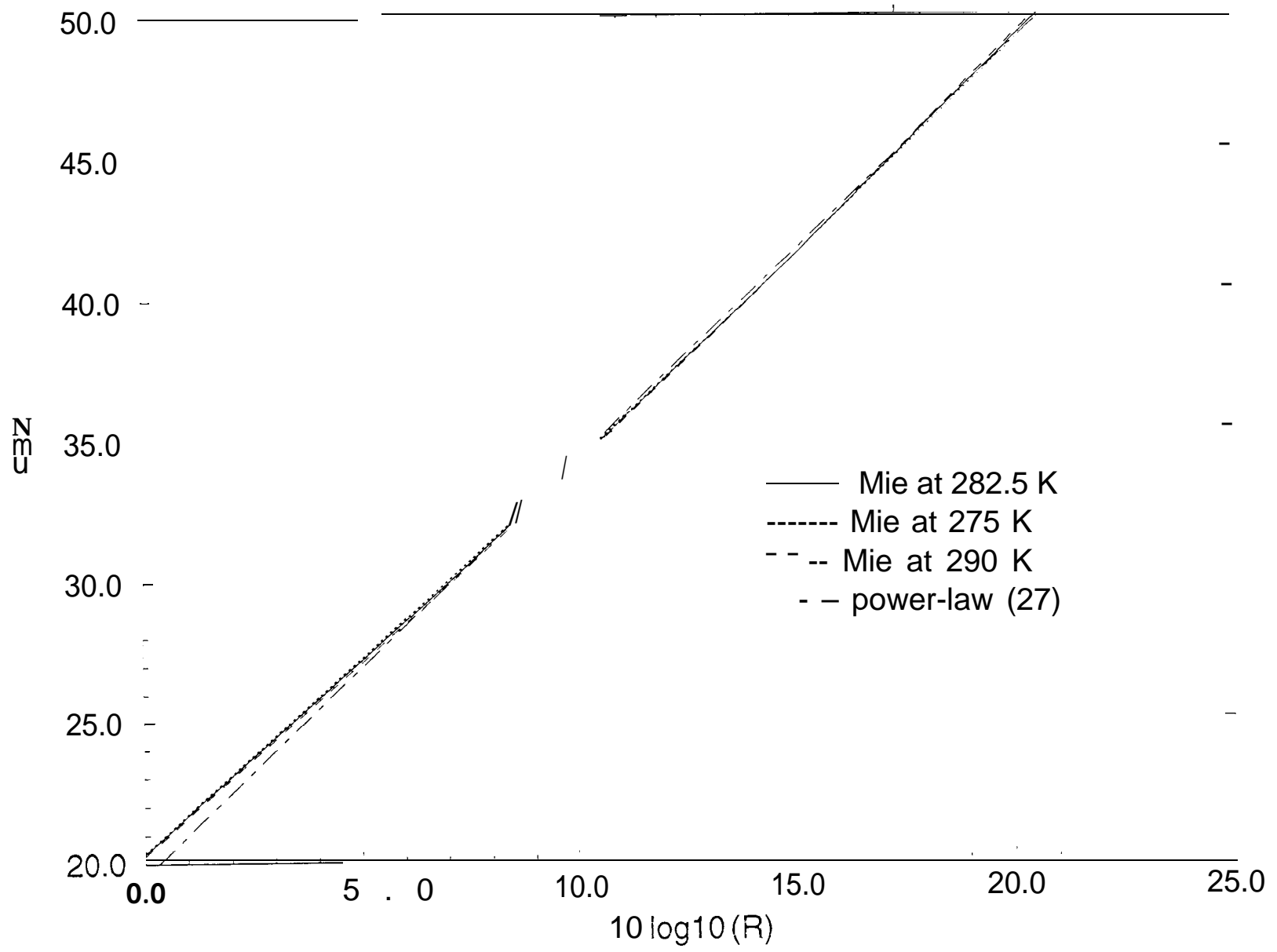
k - R

$D''=1.8, s''=0.44$



z-1?

$D''=0.8, s''=0.34$



k - R

$D''=0.8, s''=0.34$

